PVTOL global stabilisation using a nested saturation control

Rogelio Lozano, Sergio Salazar, Donovan Flores, Iván González-Hernández

PVTOL global stabilisation using a nested saturation control

Rogelio Lozano, Sergio Salazar, Donovan Flores and Iván González-Hernández

ABSTRACT

This paper presents how the nested saturation control introduced in Teel (1992) can be modified to stabilise the model of the Planar Vertical Take-Off and Landing (PVTOL) system. A particular choice of the amplitudes of the nested saturations controller is given such that global stability of the closed loop system is obtained. The proof is given in detail. Numerical simulations illustrate the performance of the proposed control algorithm.

1. Introduction

In the last decades, the PVTOL (Planar Vertical Take-Off and Landing) problem has attracted many researchers. The interest is motivated by the fact that many different configurations of aerial systems are currently used in numerous applications. The PVTOL is a challenging nonlinear system mainly because it is an under-actuated mechanical system, i.e. the number of control inputs is less than the number of degrees-of-freedom. Therefore, finding an appropriate feedback control strategy will help achieving a high level of performance.

One of the first controllers proposed for the PVTOL was introduced by Hauser et al. (1992). They showed that applying an exact input–output linearisation technique to the flight control of the VTOL leads to a system with unstable internal dynamics. They proposed a solution with an approximate input–output linearisation procedure developed for slightly non-minimum phase nonlinear systems.

The beginning of the 90s was also marked by the interest on stabilising linear systems with bounded inputs. The nested saturation control technique introduced by Teel (1992) was proposed to stabilise n integrators in cascade with a bounded input. However, it should be pointed out that it is not straightforward to apply such nested saturation approach to the PVTOL since it is a nonlinear system.

Lozano et al. (2004) and Garcia et al. (2006) proposed to use the nested saturation control to stabilise the PVTOL. The stability was ensured only when the orientation angle theta and its derivative were initially sufficiently small. The idea to use the nested saturation technique surged from the fact that when the altitude is controlled by nonlinear compensation, then the resulting subsystem from the torque input τ to the output x (the horizontal displacement) reduces to four integrators in cascade when θ is small, i.e. when $\tan\theta \approx \theta$.

The closed loop system obtained when using the controller proposed in Lozano et al. (2004) was only locally stable. Extending the proof to establish global stability of the closed loop has been hampered by the possibility of crossing the singular point $\cos\theta = 0$. The search for a global stability proof is motivated by the fact the controller based on nested saturations is relatively simple and is currently used in practice with good performance.

Nicotra et al. (2014, June) have also applied the nested saturation control to an UAV for the transportation of suspended loads. They proved stability of the equilibrium for small sway angles of the suspended load.

An almost-globally stable controller was proposed by Hua et al. (2009) using a Lyapunov approach. The results showed robustness with respect to aerodynamic drag disturbances.

A hierarchical controller was proposed for the PVTOL in Abdessameud and Tayebi (2010) for trajectory tracking in the absence of linear velocity measurements.

Aguilar (2017) presented a controller based on a combination of a PD controller and a sliding mode controller to stabilise both the horizontal and angular variables to the desired rest position. The closed loop system was proved to be locally stable provided that the initial angular rate and angular position belong to a given region where no singularity occurs.

Naldi et al. (2016) proposed a hierarchical control strategy for a miniature VTOL vehicle to track a desired trajectory globally with respect to the initial position and attitude. Their control strategy overcome the topological constraint on the orientation by using this orientation angle as a virtual input to stabilise the aircraft position. Tran et al. (2018) proposed also a control algorithm to obtain a globally stable controller for UAVs. Furthermore, their control strategy is adaptive and can deal also with unknown system parameters.

Zavala-Río et al. (2003) propose a global stabilising control design for PVTOL aircraft, with bounded inputs. This approach is based on the use of non-linear combinations of linear saturation functions bounding the thrust input and the rolling moment to arbitrary saturation limits. Their proof of stability has been extended to the case of small lateral force coupling in López-Araujo et al. (2010). A global stabilising control law is proposed for a non-minimum phase under-actuated PVTOL aircraft by Poulin et al. (2007). Their approach is based on

receding horizon control and takes into account the positiveness of the thrust and its saturation to any arbitrary level.

Both control schemes (Naldi et al., 2016; Tran et al., 2018) used the orientation angle as a virtual control input in such a way that the PVTOL model appears as fully actuated. Such virtual control is based on smooth saturation functions of the position and velocity. The first and second derivatives of the virtual control are required so that the actual orientation angle converges to the required virtual control. These derivatives are needed even if the objective is to stabilise the system at hover. A drawback of this technique is that the expressions for the first and second derivatives of the orientation virtual control input are very complex. The approach based on virtual control forces requires the thrust input to be strictly positive, since for $u = 0$ the virtual control input for θ is undefined. To avoid this singularity, the virtual force for the altitude is chosen as $F = g - \sigma(z, \dot{z}) > 0$ where g is the gravitational acceleration and σ is a smooth saturation function. Therefore the thrust control input u will satisfy $0 < u < 2g$ (neglecting the virtual control input for x). The upperbound on the trust input u may not be a problem in many situations, but this constraint on u could limit the agility of those aerial vehicle which require to perform aggressive manoeuvres. These control schemes require measurement of the acceleration signal which is often noisy.

The present paper proposes a controller which is simpler compared to those based on virtual control proposed by Naldi et al. (2016); Tran et al. (2018). The control strategy is presented in a multistage constructive procedure as follows. The torque control input τ is chosen as a nested saturation controller which, after a transient time, ensures bounds for the orientation rate $\dot{\theta}$ and angular position θ so that the orientation θ is bounded away from the singular point of 90°. We exploit the fact that provided the control inputs u and τ are bounded, the PVTOL system cannot have a finite escape time. Boundedness of $\dot{x}$ and x is established later after the altitude converges to its desired value. The control input u is based on the compensation of the nonlinearity $\cos\theta$ and therefore can only be computed after θ is bounded away from the singular point $\theta = 90°$. The bounds of the saturation functions have been modified from those proposed by Teel (1992) in order to guarantee that after an explicit finite time the orientation angle θ is constrained to evolve in an interval which does not contain the singular point $\theta = 90°$. Consequently, once θ is inside the region which is free of singularities, then the altitude can be stabilised by compensating the nonlinear term $\cos\theta$. We then resume the analysis of the nested saturation control of the torque input τ to study the boundedness and convergence of $\dot{x}$ and x. It turns out that provided some conditions on the bounds of the saturation functions we can prove that the state of the closed loop system converges to the origin. The proposed controller does not require computing the first and second derivatives of a virtual force. The controller requires only the measurements of the system state and does not require measurement of linear acceleration nor angular acceleration. The presented controller can be interpreted as an extension of nested saturation controller for n integrators in cascade including nonlinearities as the tangent function.

Aguilar et al. (2019) solve the trajectory-tracking control problem of the PVTOL aircraft under crosswind. The PVTOL is linearised by differentiating twice the system equations which is called dynamic extension. This method requires the obtained control input to be different from zero, which is often the case in practical applications. This method is based on disturbance observers designed using sliding mode techniques.

Escobar et al. (2019) focused on finding the conditions for local asymptotic stability when using a control based on feedback linearisation of the PVTOL based on dynamic extension. The domain of attraction is obtained by using a Lyapunov approach.

Hernández et al. (2020) use the immersion and invariance control technique to design a controller that globally stabilises the PVTOL aircraft system. The controller gives priority to the aircraft's altitude before controlling the lateral displacement resulting in less thrust effort and less roll moment.

Aguilar et al. (2020) present an energy shaped approach to stabilise the PVTOL aircraft, in conjunction with an exact differentiator o bserver, t o e stimate t he n on-available velocities. Asymptotic convergence is proved by applying LaSalle's theorem, assuming that the system is initialised in the interval $(-\pi/2, \pi/2)$.

This paper is organised as follows : Section 2 presents the PVTOL model. Section 3 presents the nested saturation control algorithm for the torque control input and shows that the angular rate $\dot{\theta}$ has an upperbound. Section 4 gives the upperbound on the orientation angle θ. Section 5 presents the thrust control algorithm. Section 6 shows an upperbound for the velocity $\dot{x}$. Section 7 finally shows convergence of the position x to zero. The proposed algorithm is tested in numerical simulations in Section 8. Final remarks are given in the conclusion.

2. PVTOL model

The model of the PVTOL is given by Lozano et al. (2004):

$$m\ddot{x} = u\sin\theta \tag{1}$$

$$m\ddot{z} = u\cos\theta - mg \tag{2}$$

$$\ddot{\theta} = \tau \tag{3}$$

where m is the mass, θ is the angle of the aircraft with respect to the horizontal line, g is the gravitational acceleration, x is the horizontal displacement, z is the vertical displacement. u and τ are the total thrust and torque respectively.

3. Upperbound on the orientation rate $\dot{\theta}$

In this section, we will present the nested saturation controller applied to the x-θ subsystem. We will show that after some finite time the upperbound on $\dot{\theta}$ is smaller than a given value.

The state of the $x - \theta$ subsystem is given as

$$x_1 = \frac{x}{g} \quad x_2 = \frac{\dot{x}}{g} \quad x_3 = \theta \quad x_4 = \dot{\theta} \tag{4}$$

Let us define the following variables:

$$\begin{aligned} \nu_1 &= x_3 + x_4 \\ \nu_2 &= x_2 + 2x_3 + x_4 \\ \nu_3 &= x_1 + 3x_2 + 3x_3 + x_4 \end{aligned} \tag{5}$$

consider the subsystem

$$\dot{x}_4 = \tau \tag{6}$$

$$\dot{\nu}_1 = x_4 + \tau \tag{7}$$

and the torque input given by the following nested saturation control law:

$$\tau = -\sigma_a(x_4 + \sigma_b(\nu_1 + \sigma_c(\nu_2 + \sigma_d(\nu_3)))) \tag{8}$$

where σ_a is the saturation function:

$$\sigma_a = \begin{cases} a & x > a \\ x & -a \le x \le a \\ -a & x < -a \end{cases} \tag{9}$$

Introducing (8) into (6)

$$\dot{x}_4 = -\sigma_a(x_4 + \sigma_b(w_1)) \tag{10}$$

with

$$w_1 = \nu_1 + \sigma_c(\nu_2 + \sigma_d(\nu_3)) \tag{11}$$

Assume that

$$a \ge 2b + \epsilon_1 \tag{12}$$

for some $\epsilon_1 > 0$.

Appendix 1 gives the expression for a finite time t_1 such that for some $\epsilon_1 > 0$

$$|\dot{\theta}| = |x_4| \le b + \epsilon_1 \quad \forall\, t \ge t_1 \tag{13}$$

4. Upperbound on the orientation angle θ

In this section, we will show that after some finite time θ will belong to an interval which does not include the singular point $\theta = 90^\circ$.

After $t = t_1$ and in view of (7), (8), (12) and (13), (7) reduces to

$$\dot{\nu}_1 = -\sigma_b(\nu_1 + \sigma_c(w_2)) \tag{14}$$

with

$$w_2 = \nu_2 + \sigma_d(\nu_3) \tag{15}$$

Let

$$b \ge 2c + \epsilon_2 \tag{16}$$

for $c > 0$ and some $\epsilon_2 > 0$. Appendix 2 gives the expression for a finite time t_2 such that

$$|\theta + \dot{\theta}| = |\nu_1| \le c + \epsilon_2 \quad \forall\, t \ge t_2 \tag{17}$$

Let us choose c such that

$$c + \epsilon_2 < \frac{\pi}{n+1} \tag{18}$$

for some integer $n = 3, 4, \ldots$ to be determined. From (4) and (5) it follows:

$$\dot{\theta} = -\theta + \nu_1 \tag{19}$$

Appendix 3 gives the expressions for a finite time t_3 such that

$$|\theta| \le \frac{\pi}{n} \quad \forall\, t \ge t_3 \tag{20}$$

The integer $n = 3, 4, 5, \ldots$ will be chosen later so that $(\tan\theta - \theta)$ is small enough to guarantee the stability of the overall system.

5. Thrust control input u

In this section, we present the thrust control input u which is based on nonlinear compensation.

Notice that after time t_3 the value of θ in (20) is far away from the singular points $\frac{\pi}{2}$ and $-\frac{\pi}{2}$. We can then propose the following thrust control input u:

$$u = \begin{cases} \dfrac{[-2\dot{z} - (z - z^d)]m + mg}{\cos\theta} & |\theta| < \dfrac{\pi}{n} \\ mg & \dfrac{\pi}{n} \le |\theta| \le \dfrac{\pi}{3} \\ 0 & |\theta| > \dfrac{\pi}{3} \end{cases} \tag{21}$$

where z^d is the constant desired altitude. The constant values for u above when $|\theta| > \frac{\pi}{n}$ do not play a role in the convergence analysis. However, they can be used to improve the performance of the algorithm in the presence of disturbances as will be shown in the numerical simulations.

Introducing (58) into (55) gives

$$\ddot{z} + 2\dot{z} + (z - z^d) = 0 \tag{22}$$

or

$$\begin{bmatrix} \dot{z} \\ \ddot{z} \end{bmatrix} = \begin{bmatrix} 0 & 1 \\ -1 & -2 \end{bmatrix} \begin{bmatrix} z - z^d \\ \dot{z} \end{bmatrix} \tag{23}$$

6. Upperbound on the velocity $\dot{x}$

In this section, it will be shown that the velocity $\dot{x}$ will converge to a bounded interval.

Introducing (58) into (54) and (4) gives

$$\ddot{x}_1 = \frac{\ddot{x}}{g} = \tan\theta + e_1 \tag{24}$$

where

$$e_1 = \frac{\tan\theta[-2\dot{z} - (z - z_d)]}{g} \tag{25}$$

which can be rewritten as

$$\ddot{x}_1 = \theta + e_1 + e_2 \tag{26}$$

where

$$e_2 = \tan\theta - \theta \tag{27}$$

Thus, from (54) and (57), the subsystem for $x, \dot{x}, \theta$ and $\dot{\theta}$ is given by (see (4))

$$\begin{aligned} \dot{x}_1 &= x_2 \\ \dot{x}_2 &= x_3 + e \\ \dot{x}_3 &= x_4 \\ \dot{x}_4 &= \tau \end{aligned} \tag{28}$$

with

$$e = e_1 + e_2 \tag{29}$$

From (5)

$$\begin{aligned}\dot{\nu}_2 &= \dot{x}_2 + 2\dot{x}_3 + \dot{x}_4 \\ &= x_3 + e + 2x_4 + \tau \\ &= x_4 + \nu_1 + e + \tau\end{aligned} \tag{30}$$

Taking into account (13) and (17), (8) reduces to

$$\tau = -x_4 - \nu_1 - \sigma_c(\nu_2 + \sigma_d(\nu_3))$$

Introducing the above into (30) leads to

$$\dot{\nu}_2 = -\sigma_c(\nu_2 + \sigma_d(\nu_3)) + e \tag{31}$$

Choose d so that for some $\epsilon_3 > 0$

$$c \geq 3d + \epsilon_3 \tag{32}$$

Appendix 4 gives the expression for a finite time t_4 such (see (25))

$$|e_1| \leq \frac{d}{6} \quad \forall\, t \geq t_4 \tag{33}$$

The integer $n \geq 3$ will be chosen such that for some $k > 0$ the following holds (see (20) and (27))

$$\begin{aligned}|e_2| &= |\tan\theta - \theta| \\ &\leq k|\theta| \\ &\leq k\frac{\pi}{n} \leq \frac{d}{6}\end{aligned} \tag{34}$$

Introducing (33) and (34) into (29)

$$\begin{aligned}|e| &\leq |e_1| + |e_2| \\ &\leq \frac{d}{3}\end{aligned} \tag{35}$$

Using (31), (32) and the above, the expression for a finite time t_5 is given in Appendix 5 such that

$$|\nu_2| \leq 2d + \epsilon_3 \quad \forall\, t \geq t_5 \tag{36}$$

Therefore (31) reduces to

$$\dot{\nu}_2 = -\nu_2 - \sigma_d(\nu_3) + e \tag{37}$$

7. Convergence of the position *x*

In this section, we will prove that the horizontal displacement x converges to zero.

From (5) and using (28) and (8)

$$\begin{aligned}\dot{\nu}_3 &= \dot{x}_1 + 3\dot{x}_2 + 3\dot{x}_3 + \dot{x}_4 \\ &= x_2 + 3x_3 + 3e + 3x_4 + \tau \\ &= x_4 + \nu_1 + \nu_2 + 3e + \tau \\ &= -\sigma_d(\nu_3) + 3e\end{aligned} \tag{38}$$

From (35) and (38) a finite time t_6 is given in Appendix 6 such that

$$|\nu_3| \leq d \quad \forall\, t \geq t_6$$

From (4), (5) and (28) we get

$$\dot{x}_3 = -x_3 + \nu_1 \tag{39}$$

$$\dot{\nu}_1 = -\nu_1 - \nu_2 - \nu_3 \quad \text{(see (14) and (15))} \tag{40}$$

$$\dot{\nu}_2 = -\nu_2 - \nu_3 + e \quad \text{(see (37))} \tag{41}$$

$$\dot{\nu}_3 = -\nu_3 + 3e \quad \text{(see (38))} \tag{42}$$

Define

$$X^T = \begin{bmatrix} x_3 & \nu_1 & \nu_2 & \nu_3 \end{bmatrix} \tag{43}$$

$$b^T = \begin{bmatrix} 0 & 0 & 1 & 3 \end{bmatrix} \tag{44}$$

and

$$A = \begin{bmatrix} -1 & 1 & 0 & 0 \\ 0 & -1 & -1 & -1 \\ 0 & 0 & -1 & -1 \\ 0 & 0 & 0 & -1 \end{bmatrix} \tag{45}$$

Therefore (39) through (42) can be rewritten as

$$\dot{X} = AX + be \tag{46}$$

The state space representation above has a system matrix A that is stable with 4 eigenvalues located at -1. Recall that $e = e_1 + e_2$ (see 29) where e_1 converges to zero, (see (22) and (25)). Furthermore $|e_2| \leq k|\theta| = k|x_3|$ for a value of 'k' that has to be determined so that it satisfies (34) and is simultaneously small enough such that (46) remains stable.

The values for k and n such that (46) is a stable system could be obtained by using a Lyapunov function $X^T PX$ where $P > 0$ is the solution of the Lyapunov equation $A^T P + PA = -Q$ for some $Q > 0$. Nevertheless, for simplicity we will proceed as follows.

From (20) and (22) it follows that e_1 in (25) converges to zero. Since A in (46) is a stable matrix, the contribution of e_1 in X will also converge to zero. From (34) $|e_2| \leq k|\theta|$. Thus, following the procedure developed in Appendix 3, we can prove using (42) that there exists a finite time t_7 such that

$$|\nu_3| \leq 3k|\theta| + \epsilon \quad \forall\, t \geq t_7 \tag{47}$$

for some $\epsilon > 0$.

Similarly, using (41), there exists a finite time t_8 such that

$$|\nu_2| \leq 4k|\theta| + 2\epsilon \quad \forall\, t \geq t_8 \tag{48}$$

Similarly, from (40) it follows that there exists t_9 such that

$$|\nu_1| \leq 7k|\theta| + 3\epsilon \quad \forall\, t \geq t_9 \tag{49}$$

Let us assume that k also satisfies

$$\mu^2 = 1 - 7k > 0 \tag{50}$$

Finally from (4) and (39)

$$\dot{\theta} = -\theta + \nu_1 \tag{51}$$

Let $V = \frac{1}{2}\theta^2$ then, using (49)

$$\dot{V} = \theta\dot{\theta} = \theta(-\theta + \nu_1)$$

$$
\begin{aligned}
&\leq -\theta^2 + 7k\theta^2 + 3|\theta|\epsilon \\
&\leq -\mu^2\theta^2 + 2\left(\frac{\mu|\theta|}{2}\right)\left(\frac{3\epsilon}{\mu}\right) \\
&\leq -\frac{3}{4}\mu^2\theta^2 + \frac{9\epsilon^2}{\mu^2} \\
&\leq -\frac{3}{2}\mu^2 V + \frac{9\epsilon^2}{\mu^2} \qquad (52)
\end{aligned}
$$

Since ϵ can be chosen arbitrarily small it follows from the above that $V \to 0$ and therefore $\theta \to 0$. From (51) and (4), we conclude that $x_3 \to 0$ and $x_4 \to 0$. From (47)–(49) it follows that $\nu_1 \to 0$, $\nu_2 \to 0$ and $\nu_3 \to 0$. From (5), $x_2 \to 0$ and $x_1 \to 0$. From (4) it finally follows $x \to 0, \dot{x} \to 0, \theta \to 0, \dot{\theta} \to 0$.

The constraints required for n and k are given in (34) and (50). Appendix 6 proves that for $n = 9$ and $k = 0.0424$ both constraints are verified. Notice that $\frac{\pi}{9} = 20^\circ$.

Finally let us summarise the constraints on the saturation upperbounds a, b, c and d. See (12), (16), (18), (32) and (34)

$$
\begin{aligned}
a &\geq 2b + \epsilon_1 \\
b &\geq 2c + \epsilon_2 \\
0.1\pi &\geq c + \epsilon_2 \qquad (53) \\
&\geq 3d + \epsilon_2 + \epsilon_3 \\
&\geq 0.085\pi + \epsilon_2 + \epsilon_3
\end{aligned}
$$

The choice of the parameter a depends on the upperbound of the torque control input τ. In practice the higher the value of a the faster the angular rate $\dot{\theta}$ will decrease after a disturbance and therefore the aerial vehicle attitude will be more robust to disturbances. Nevertheless, when the parameter a is chosen too high, it is common that mechanical vibrations appear. The parameters b, c and d are determined by the choice of the parameter a. Concerning the parameters ϵ_i, they have been introduced so that the corresponding state variables are smaller than a given bound in finite time. The higher the value of ϵ_i the shorter the corresponding time period t_i will be.

8. Numerical simulation results

In this section, we will present a comparison between the proposed control algorithm and the control strategy introduced in Lozano et al. (2004). We will also show the robustness properties of the proposed algorithm with respect to plant parameter changes. We will consider that the PVTOL is represented by the following equations:

$$m\ddot{x} = u\sin\theta \qquad (54)$$

$$m\ddot{z} = u\cos\theta - mg \qquad (55)$$

$$\dot{\theta} = \theta_1 + w_p \qquad (56)$$

$$\dot{\theta}_1 = k\tau \qquad (57)$$

where w_p is a perturbation given as follows:

$$w_p = \begin{cases} 2.3 & 15s \leq t \leq 16s \\ 0 & \text{otherwise} \end{cases} \qquad (58)$$

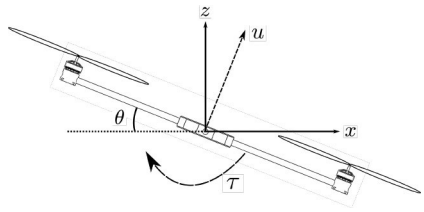

Figure 1. PVTOL configuration.

Figure 2 presents the comparison between the control algorithm proposed in the present paper and the algorithm in Lozano et al. (2004). This figure presents (a) the displacement x, (b) the control input u, (c) the orientation angle theta and (d) the altitude z. The initial conditions have been chosen as $z(0) = 0, \theta(0) = 0, x(0) = 0$.

We have introduced a disturbance at time 15 s in the orientation rate $\dot{\theta}$. As can be seen in Figure 2 the disturbance produces a much smaller displacement x in the case of the proposed algorithm and the displacement x takes much less time to come back to the origin. Figure 2(b) shows that the thrust input is smaller for the proposed algorithm. The angular displacement in Figure 2(c) is just a little smaller for our algorithm. Figure 2(d) shows that the price to be paid for obtaining the above advantages with the proposed algorithm is to reduce the altitude of the PVTOL during a few seconds.

Concerning the robustness of the proposed algorithm with respect to changes in the plant parameter, we have considered two different plant parameters: the mass m and the torque control gain k.

We have used the same initial conditions as before as well as the same disturbance in the angular orientation rate $\dot{\theta}$. Figure 3 shows the performance of the proposed controller when the plant mass m increases or decreases 20%. As can be seen a change in the plant m produces an error in between the altitude and the desired altitude. The rest of the closed-loop system behaves with no significant changes.

Figure 4 shows the performance of the proposed controller when the torque gain k increases or decreases 20%. As can be seen when k increases the closed loop system behaves well. However, when k decreases the system requires a larger control input and more time to converge.

9. Conclusion

This paper addressed the problem of obtaining a simple control algorithm for the PVTOL. The nonlinearity of the PVTOL has been an obstacle for obtaining stable controllers. Since the PVTOL can be approximated by four integrators in cascade, the nested saturations controller proposed in Teel (1992) has been currently used to control the PVTOL. However, no proof of stability of the closed loop has been obtained in the past. This paper has shown that a particular choice of the amplitudes of the saturations involved in the technique in Teel (1992) allows for the proof of global stability of the closed loop. The performance of the proposed controller is shown in numerical simulations.

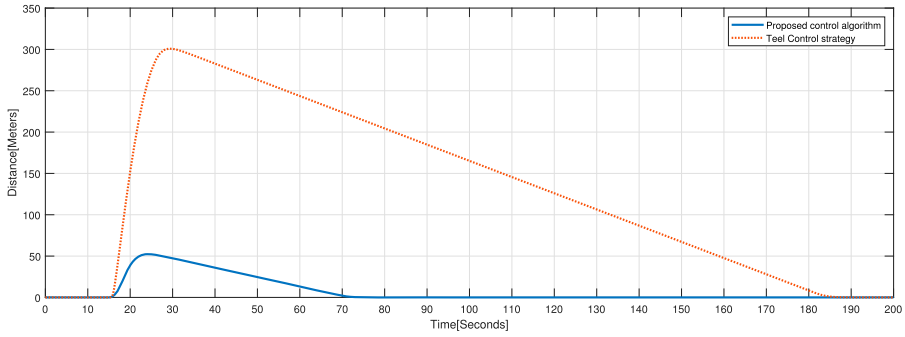

(a) x-position

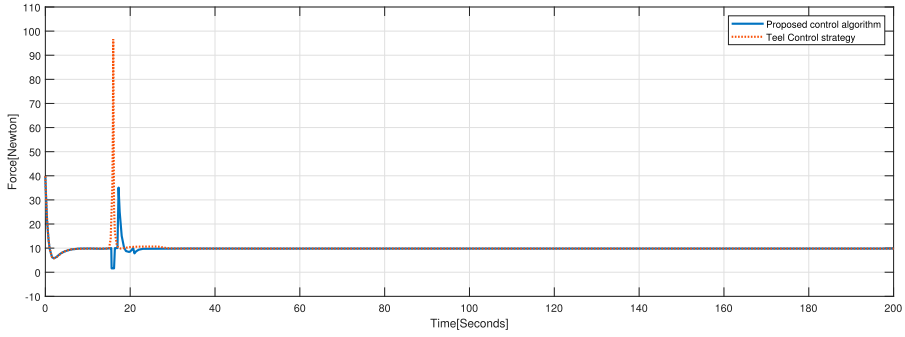

(b) u control input

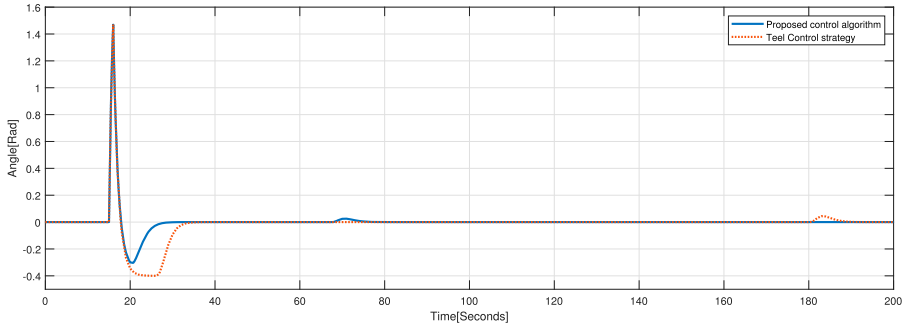

(c) θ orientation angle

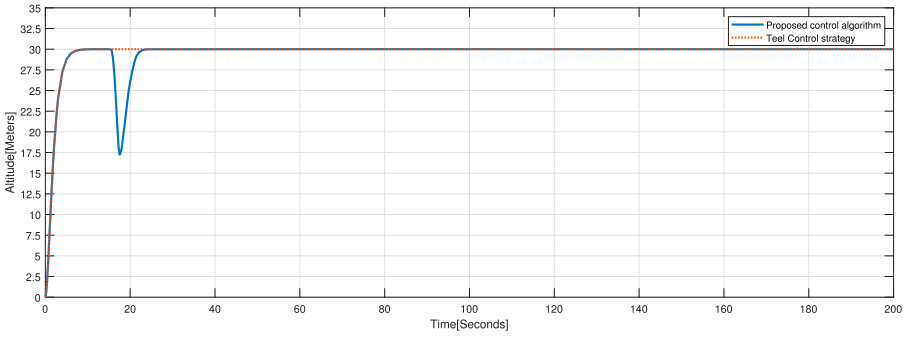

(d) z-position

Figure 2. Comparison between the proposed control algorithm and the original Teel's strategy when a disturbance is introduced at time 15 s: (a) *x*-position, (b) *u* control input, (c) θ orientation angle and (d) *z*-position.

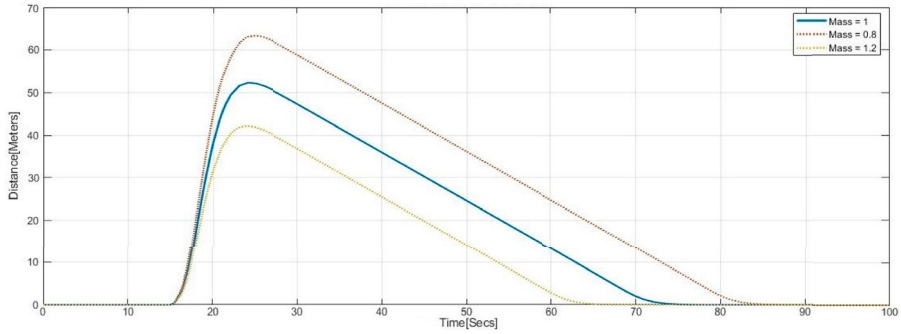

(a) x-position

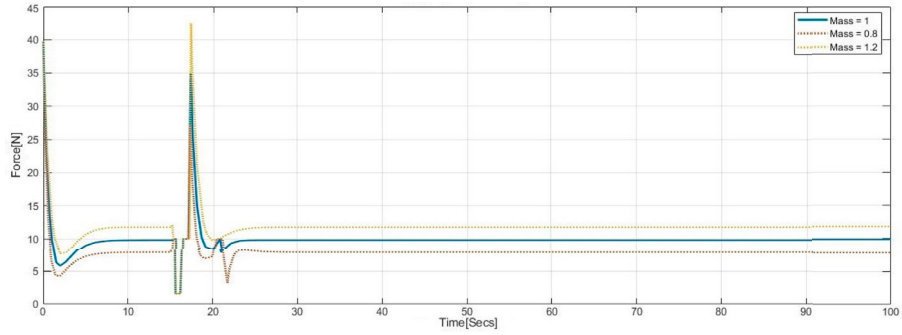

(b) u control input

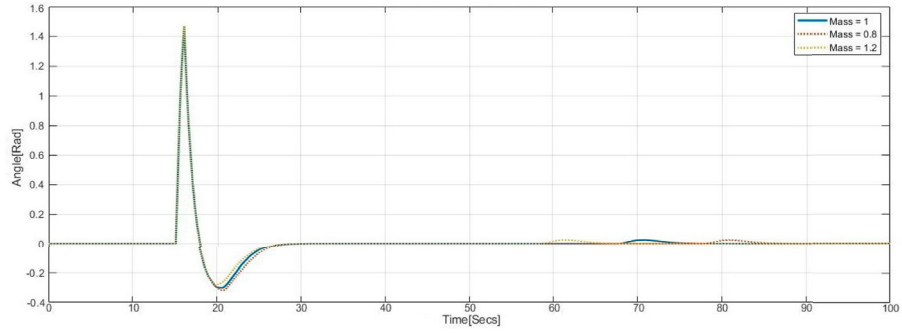

(c) θ orientation angle

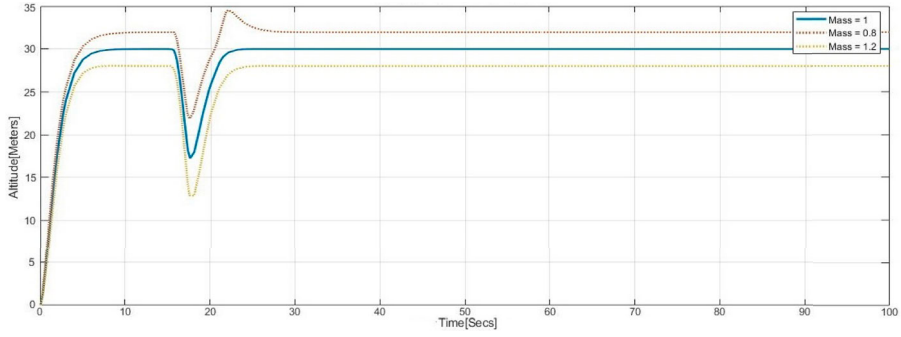

(d) z-position

Figure 3. Robustness of the proposed algorithm with respect to variations of the mass value m: (a) x-position, (b) u control input, (c) θ orientation angle and (d) z-position.

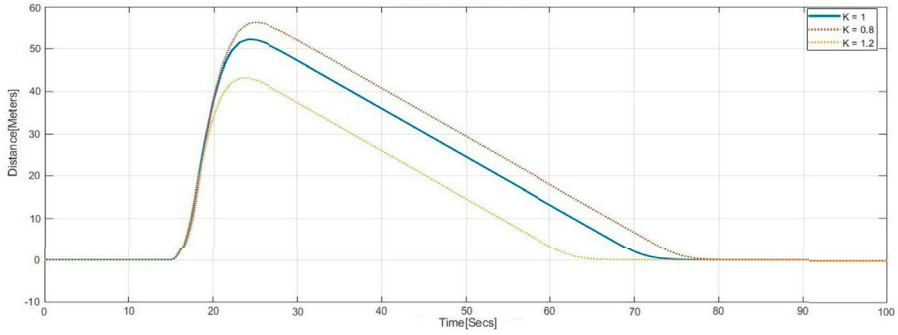

(a) x-position

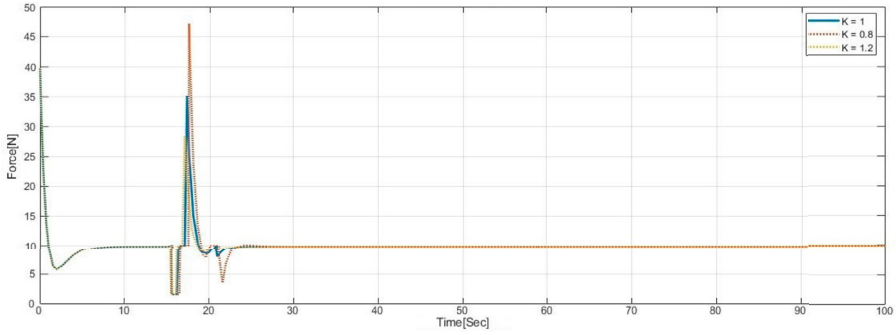

(b) u control input

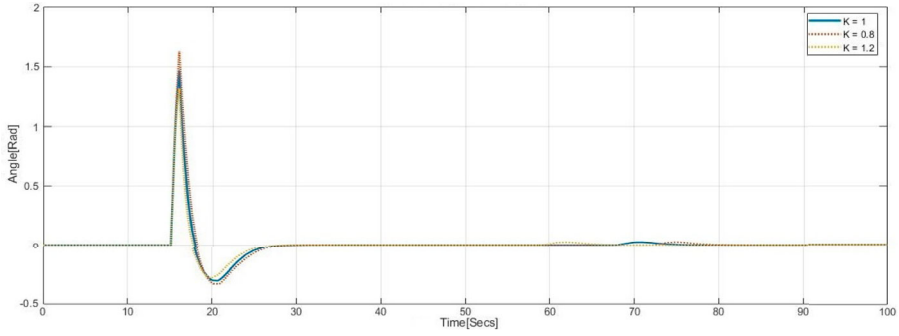

(c) θ orientation angle

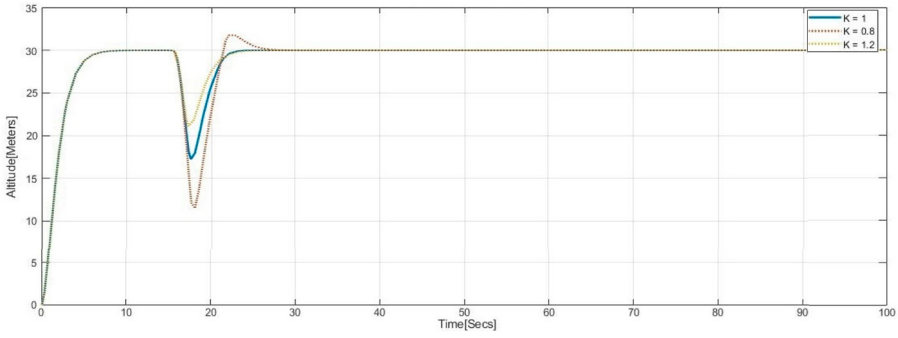

(d) z-position

Figure 4. Robustness of the proposed algorithm with respect to variations of the gain value *k*: (a) *x*-position, (b) *u* control input, (c) θ orientation angle, (d) *z*-position.

References

Abdessameud, A., & Tayebi, A. (2010). Global trajectory tracking control of VTOL-UAVs without linear velocity measurements. *Automatica*, *46*, 1053–1059. https://doi.org/10.1016/j.automatica.2010.03.010

Aguilar, C. (2017). Stabilization of the PVTOL aircraft based on a sliding mode and a saturation function. *International Journal of Robust and Nonlinear Control*, *27*(5), 843–859. https://doi.org/10.1002/rnc.3601

Aguilar, C., Sira-Ramirez, H., Suarez, M. S., & Garrido, R. (2019, May). Robust trajectory-tracking control of a PVTOL under crosswind. *Asian Journal of Control*, *21*(3), 1293–1306. https://doi.org/10.1002/asjc.v21.3

Aguilar, C., Suarez, M. S., Meda, J., Gutierrez, O., Merlo, C., & Martinez, J. A. (2020). A simple approach to regulate a PVTOL system using matching conditions. *Journal of Intelligent and Robotic Systems*, *98*, 511–524. https://doi.org/10.1007/s10846-019-01087

Escobar, J. C., Lozano, R., & Bonilla Estrada, M. (2019). PVTOL control using feedback linearisation with dynamic extension. *International Journal of Control*, 1–10. https://doi.org/10.1080/00207179.2019.1676468

Garcia, P. C., Lozano, R., & Dzul, A. E. (2006). *Modelling and control of mini-flying machines*. Springer Science & Business Media.

Hauser, J., Sastry, S., & Meyer, G. (1992). Nonlinear control design for slightly non-minimum phase systems: application to V/STOL aircraft. *Automatica*, *28*(4), 665–679. https://doi.org/10.1016/0005-1098(92)90029-F

Hernández, F., Santibáñez, V., & Jurado, F. (2020). Priority altitude PVTOL aircraft control via immersion and invariance. *International Journal of Control*, *93*(10), 2290–2301. https://doi.org/10.1080/00207179.2018.1554269

Hua, M. D., Hamel, T., Morin, P., & Samson, C. (2009). A control approach for thrust-propelled underactuated vehicles and its application to VTOL drones. *IEEE Transactions on Automatic Control*, *54*(8), 1837–1853. https://doi.org/10.1109/TAC.2009.2024569

López-Araujo, D. J., Zavala-Río, A., Fantoni, I., Salazar, S., & Lozano, R. (2010). Global stabilisation of the PVTOL aircraft with lateral force coupling and bounded inputs. *International Journal of Control*, *83*(7), 1427–1441. https://doi.org/10.1080/00207171003758778

Lozano, R., Castillo, P., & Dzul, A. (2004). Global stabilization of the PVTOL: real-time application to a mini-aircraft. *IFAC Proceedings Volumes*, *37*(21), 235–240. https://doi.org/10.1016/S1474-6670(17)30474-3

Naldi, R., Furci, M., Sanfelice, R. G., & Marconi, L. (2016). Robust global trajectory tracking for underactuated VTOL aerial vehicles using inner-outer loop control paradigms. *IEEE Transactions on Automatic Control*, *62*(1), 97–112. https://doi.org/10.1109/TAC.2016.2557967

Nicotra, M. M., Garone, E., Naldi, R., & Marconi, L. (2014, June). Nested saturation control of an uav carrying a suspended load. In *2014 American Control Conference*, IEEE (pp. 3585–3590).

Poulin, G., Chemori, A., & Marchand, N. (2007). Minimum energy oriented global stabilizing control of the PVTOL aircraft. *International Journal of Control*, *80*(3), 430–442. https://doi.org/10.1080/00207170601069505

Teel, A. R. (1992). Global stabilization and restricted tracking for multiple integrators with bounded controls. *Systems & Control Letters*, *18*(3), 165–171. https://doi.org/10.1016/0167-6911(92)90001-9

Tran, T. T., Ge, S. S., & He, W. (2018). Adaptive control of a quadrotor aerial vehicle with input constraints and uncertain parameters. *International Journal of Control*, *91*(5), 1140–1160. https://doi.org/10.1080/00207179.2017.1309572

Zavala-Río, A., Fantoni, I., & Lozano, R. (2003). Global stabilization of a PVTOL aircraft model with bounded inputs. *International Journal of Control*, *76*(18), 1833–1844. https://doi.org/10.1080/00207170310001637147.

Appendices

Appendix 1. Bound for $x_4 = \dot{\theta}$

Let

$$V_1 = \frac{1}{2}x_4^2 \tag{A1}$$

Introducing (10) into above

$$\dot{V}_1 = x_4\dot{x}_4 = -x_4\sigma_a(x_4 + \sigma_b(w_1)) \tag{A2}$$

If

$$|x_4| > b + \epsilon_1 \tag{A3}$$

it follows that

$$\dot{V}_1 \leq -(b+\epsilon_1)\epsilon_1 \tag{A4}$$

or

$$\dot{V}_1 + (b+\epsilon_1) \leq 0 \tag{A5}$$

Integrating

$$V_1 - V_1(0) + (b+\epsilon_1)\epsilon_1 t \leq 0 \tag{A6}$$

or

$$V_1 \leq V_1(0) - (b+\epsilon_1)\epsilon_1 t \tag{A7}$$

Define t_1 such that the RHS of the above satisfies

$$V_1(0) - (b+\epsilon_1)\epsilon_1 t_1 = \frac{1}{2}(b+\epsilon_1)^2 \tag{A8}$$

thus

$$t_1 = \frac{V_1(0)}{(b+\epsilon_1)\epsilon_1} - \frac{(b+\epsilon_1)}{2\epsilon_1} \tag{A9}$$

Therefore

$$|x_4| \leq b + \epsilon_1 \quad \forall\, t \geq t_1 \tag{A10}$$

then, for $t \geq t_1$, (10) reduces to

$$\dot{x}_4 = -x_4 - \sigma_b(w_1) \tag{A11}$$

thus

$$\dot{V}_1 = x_4\dot{x}_4 = -x_4(x_4 + \sigma_b(w_1)) \tag{A12}$$

Notice that when $|x_4| > b + \epsilon_1$ it follows that $\dot{V}_1 < 0$, and V_1 will decrease. So if $|x_4| \leq b + \epsilon_1$ at some time, it will remain so from then on.

Appendix 2. Bound for $\nu_1 = \theta + \dot{\theta}$

Let

$$V_2 = \frac{1}{2}\nu_1^2 \tag{A13}$$

$$\dot{V}_2 = \nu_1\dot{\nu}_1 = -\nu_1\sigma_b(\nu_1 + \sigma_c(w_2))$$

If $|\nu_1(t_1)| > c + \epsilon_2$ it follows from (14) that for $t \geq t_1$

$$\dot{V}_2 \leq -(c+\epsilon_2)\epsilon_2 \tag{A14}$$

or

$$\dot{V}_2 + (c+\epsilon_2)\epsilon_2 \leq 0 \tag{A15}$$

Integrating from $t = t_1$

$$V_2 - V_2(t_1) + (c+\epsilon_2)\epsilon_2(t - t_1) \leq 0 \tag{A16}$$

or

$$V_2 \leq V_2(t_1) - (c+\epsilon_2)\epsilon_2(t - t_1) \tag{A17}$$

Define t_2 such that the RHS of the above satisfies

$$V_2(t_1) - (c+\epsilon_2)\epsilon_2(t_2 - t_1) = \frac{(c+\epsilon_2)^2}{2} \tag{A18}$$

thus

$$t_2 = t_1 + \frac{V_2(t_1)}{(c+\epsilon_2)\epsilon_2} - \frac{(c+\epsilon_2)}{2\epsilon_2} \tag{A19}$$

Therefore

$$|\nu_1| \leq c + \epsilon_2 \quad \forall\, t \geq t_2 \tag{A20}$$

Appendix 3. Bound for θ

From (19)

$$\dot{\theta} = -\theta + \nu_1 \tag{A21}$$

Let

$$V_3 = \frac{1}{2}\theta^2 \tag{A22}$$

Introducing (A20)

$$\begin{aligned}\dot{V}_3 &= \theta\dot{\theta} = \theta[-\theta + \nu_1] \\ &= -\theta^2 + \theta\nu_1 \leq -\theta^2 + |\theta|(c + \epsilon_2)\end{aligned} \tag{A23}$$

From (18)

$$(c + \epsilon_2) \leq \frac{\pi}{n+1} \tag{A24}$$

Assume that $|\theta| \geq \frac{\pi}{n}$, then

$$\begin{aligned}\dot{V}_3 &\leq |\theta|\left[\frac{\pi}{n+1} - |\theta|\right] \leq |\theta|\left[\frac{\pi}{n+1} - \frac{\pi}{n}\right] = |\theta|\left[-\frac{\pi}{n(n+1)}\right] \\ &\leq -|\theta|\frac{\pi}{n(n+1)} \leq -\frac{\pi^2}{n^2(n+1)}\end{aligned} \tag{A25}$$

or

$$\dot{V}_3 + \frac{\pi^2}{n^2(n+1)} \leq 0 \tag{A26}$$

Integrating from $t = t_2$

$$V_3 - V_3(t_2) + \frac{\pi^2}{n^2(n+1)}(t - t_2) \leq 0 \tag{A27}$$

or

$$V_3 \leq V_3(t_2) - \frac{\pi^2}{n^2(n+1)}(t - t_2) \tag{A28}$$

Let t_3 be such that the RHS of the above satisfies

$$V_3(t_2) - \frac{\pi^2}{n^2(n+1)}(t_3 - t_2) = \frac{1}{2}\left(\frac{\pi}{n}\right)^2 \tag{A29}$$

Then

$$t_3 = t_2 + \frac{V_3(t_2)n^2(n+1)}{\pi^2} - \frac{(n+1)}{2} \tag{A30}$$

Thus

$$|\theta| \leq \frac{\pi}{n} \quad \forall\, t \geq t_3 \tag{A31}$$

Appendix 4. Bound for e_1 in (25)

Consider (23) and define

$$Z^T = \begin{bmatrix} z - z^d & \dot{z} \end{bmatrix} \quad \text{and} \quad \bar{A} = \begin{bmatrix} 0 & 1 \\ -1 & -2 \end{bmatrix} \tag{A32}$$

then the Lyapunov equation

$$\bar{A}^T P + P\bar{A} = -Q \tag{A33}$$

holds for

$$P = \begin{bmatrix} 3 & 1 \\ 1 & 1 \end{bmatrix} > 0 \quad \text{and} \quad Q = 2I_2 \tag{A34}$$

Let

$$V = Z^T P Z \tag{A35}$$

then using (23) and (A32) – (A35)

$$\begin{aligned}\dot{V} &= Z^T\bar{A}^T P Z + Z^T P\bar{A} Z \\ &= -Z^T Q Z = -2\|Z\|^2 \\ &\leq -\alpha V\end{aligned} \tag{A36}$$

with

$$\alpha = \frac{2}{\lambda_{\max} P} \tag{A37}$$

thus

$$\dot{V} \leq -\alpha V \tag{A38}$$

Let

$$\dot{W} = -\alpha W \tag{A39}$$

with

$$W(0) = V(0) \tag{A40}$$

Since $\dot{V} \leq \dot{W}$

$$V \leq W = V(0)e^{-\alpha t} \tag{A41}$$

From (10) and (25) it follows that

$$|e_1|^2 \leq k_1^2(|\dot{z}|^2 + |z - z_d|^2) \tag{A42}$$

with

$$k_1 = \frac{6\tan\left(\frac{\pi}{3}\right)}{g} \tag{A43}$$

From (A34) and (A35)

$$\begin{aligned}|\dot{z}|^2 + |z - z_d|^2 &\leq \frac{Z^T P Z}{\lambda_{\min} P} \\ &= \frac{V}{\lambda_{\min} P} \\ &\leq \frac{W}{\lambda_{\min} P} \\ &\leq \frac{V(0)e^{-\alpha t}}{\lambda_{\min} P}\end{aligned} \tag{A44}$$

Let $t = t_4$ be such that

$$e^{-\alpha t_4} = \frac{\lambda_{\min} P}{V(0)k_1^2}(\frac{d}{6})^2 \tag{A45}$$

Introducing the above into (A44) and (A42) leads to (33), i.e.

$$|e_1| \leq \frac{d}{6} \tag{A46}$$

Appendix 5. Bound for ν_2

Define

$$V = \frac{1}{2}\nu_2^2 \tag{A47}$$

then using (31)

$$\begin{aligned}\dot{V} &= \nu_2\dot{\nu}_2 \\ &= -\nu_2[\sigma_c(\nu_2 + \sigma_d(\nu_3)) + e]\end{aligned} \tag{A48}$$

If

$$|v_2| \geq 2d + \epsilon_3 \tag{A49}$$

then from (32) and (35)

$$\dot{V} \leq -(2d + \epsilon_3)\left(\frac{2d}{3} + \epsilon_3\right) \tag{A50}$$

Integrating and proceeding as in appendices 1 and 2 we conclude that there exists a f i nite time t_5 such that (36) is satisfied.

Appendix 6. Choice of *k* and *n*

Consider $n = 9$. From (34) we have that for $\bar{\theta} = \frac{\pi}{9} = 0.3491 = 20^\circ$

$$\begin{aligned} |e_2| &= \tan\frac{\pi}{9} - \frac{\pi}{9} \\ &= 0.3639 - 0.3491 \\ &= 0.0148 \leq 0.3491k \end{aligned} \tag{A51}$$

which implies $k \geq 0.0424$

On the other hand (50) requires

$$k < \frac{1}{7} = 0.1428 \tag{A52}$$

Therefore $k = 0.0424$ verifies both constraints.

Notice that $\tan\theta - \theta$ is a strictly increasing function and the result will hold for values of $|\theta|$ smaller than $\frac{\pi}{9}$.